Open Access Article

# MOLECULAR DOCKING, SYNTHESIS, CHARACTERIZATION AND ADME STUDIES OF SOME NEW FIVE-MEMBER RING HETEROCYCLIC COMPOUNDS WITH IN VITRO ANTIPROLIFERATIVE EVALUATION.

**Kanar M. Alawad**
[1]Department of Pharmacy, AL-Rasheed University College, Baghdad-Iraq,
kanar.muthana93@gmail.com

**Monther F. Mahdi**
Department of Pharmaceutical Chemistry, College of Pharmacy, Mustansiriyah university, Baghdad-Iraq.

**Ayad M.R. Raauf**
Department of Pharmaceutical Chemistry, College of Pharmacy, Mustansiriyah university, Baghdad-Iraq.

**Abstract:**

A series of pyrazoline, Isoxazoline, and amide derivatives bearing nabumetone moiety were designed, synthesized, and primarily evaluated (*In Vitro*) for their cytotoxic activity against lung (A549). Nabumetone is a nonsteroidal anti-inflammatory (NSAID) prodrug. Chalcone derivative of nabumetone; compound (1) synthesized by Claisen-Schmidt condensation reaction, and then, the intermediate compounds (1a-e) were synthesized by incorporating pyrazoline, and Isoxazoline pharmacophore into compound (1). Amide derivatives synthesized to develop the final compounds (2a-e). Melting point, and FT-IR spectra used to characterize all the synthesized compounds, and confirmed by $^{1}$H-NMR, and $^{13}$C-NMR spectroscopy. Molecular docking software (GOLD suite *v.* 5.7.1) were used before synthesis to check the selectivity for EGFR. Precisely compounds (1e & 2e) with EGFR receptor showed the highest PLP fitness value of (92.07 & 97.11) as compared to erlotinib reference drug that give PLP fitness of (94.84). $IC_{50}$ values for the synthesized compounds showed that compound (2e) give 21.62 µM against A549 cancer cell line as compared to erlotinib that give $IC_{50}$ value of (24.6) µM. Finally, *in silico* studies including ADME studies, were The pharmacokinetics of the designed compounds were predicted using the SwissADME service. The results show that all the compounds expected passively and highly absorbed from the GIT except (1e& 2e) which are poorly absorbed from the GIT. Further, all designed compounds satisfied the Lipinski rule of five.

**KEYWORDS:** Nabumetone, Pyrazoline, Isoxazoline, Docking Study, ADME.

**抽象的**：

设计、合成了一系列带有萘丁酮部分的吡唑啉、异恶唑啉和酰胺衍生物，并初步评估了（体外）它们对肺 (A549) 的细胞毒活性。萘丁美酮是一种非甾体抗炎 (NSAID) 前药。萘丁酮

Received: July 02, 2021 / Revised: August 22, 2021 / Accepted: September 11, 2021 / Published: September 29, 2021
About the authors Kanar M. Alawad
Corresponding author- Email: kanar.muthana93@gmail.com

的查耳酮衍生物；通过克莱森-施密特缩合反应合成化合物(1)，然后将吡唑啉和异恶唑啉药效团引入化合物(1)中合成中间体化合物(1a-e)。合成酰胺衍生物以开发最终化合物 (2a-e)。熔点和 FT-IR 光谱用于表征所有合成的化合物，并通过 1H-NMR 和 13C-NMR 光谱证实。在合成前使用分子对接软件（GOLD 套件 v. 5.7.1）检查 EGFR 的选择性。与提供 (94.84) 的 PLP 适合度的厄洛替尼参考药物相比，具有 EGFR 受体的精确化合物 (1e 和 2e) 显示出最高的 PLP 适合度值 (92.07 和 97.11)。合成化合物的 IC50 值表明，与提供 (24.6) μM 的 IC50 值的厄洛替尼相比，化合物 (2e) 对 A549 癌细胞系产生了 21.62 μM。最后，包括 ADME 研究在内的计算机模拟研究使用 SwissADME 服务预测了设计化合物的药代动力学。结果表明，除了(1e&2e)，从GIT中吸收较差的所有化合物预期从GIT中被动且高度吸收。此外，所有设计的化合物都满足五的 Lipinski 规则。

关键词：萘丁美酮，吡唑啉，异恶唑啉，对接研究，ADME。

**Introduction:**

The word "cancer" refers to a category of diseases caused by internal or external factors. Cancer is a condition characterized by abnormal cell proliferation. It may begin in any area of the body, and as the disease progresses, the primary tumor develops into a malignant tumor, which then spreads to other areas of the body [(1)]. Cancer can be treated by surgery which is considered as a first line therapy, radiotherapy can be also used with surgery, cytotoxic chemotherapy which includes many drug classes such as DNA-alkylating agents, antimetabolites and others. Cytotoxic agents affect the rapidly dividing cells including the normal cells that results in many side effects [(2)]. These agents are considered to be mutagenic, teratogenic, and carcinogenic to humans, and are mostly used in chemotherapy for their ability to destroy cancerous cells. As a result of their non-selectivity, they affect both cancer and normal cells, causing well-documented side effects [(3)]. A major challenge for anticancer agents is to design new agents that will inhibit cancer cells more selectively in order to avoid adverse effects on healthy normal cells [(4)]. New types of drugs have appeared recently that attack cancer cells with high selectivity, resulting in less side effects than conventional cytotoxic drugs [(5)]. Currently, researchers are concentrating their efforts on developing novel anticancer drugs and heterocyclic compounds that have been extensively studied for this purpose [(6)]. Pyrazoline, Isoxazoline and many other heterocycles are synthesized from α,β-unsaturated carbonyl (chalcone) (1) [(7)]. Chalcones also has a broad variety of biological functions, including anticancer [(8)], xanthine oxidase inhibitors [(9)], antianxiety, antidepressant, analgesic, antimalarial, antifungal, antibacterial, anti-inflammatory, antiangiogenic properties [(10)]. Heterocyclic compounds such as pyrazole (2) and Isoxazole (3) have a broad range of biological activities which include: antimicrobial, anticonvulsant, anticancer, anti-inflammatory, and analgesic effects, antiviral, antidepressant, among others [(11-13)]. Therefore,

chalcone and a series of new heterocyclic compounds (pyrazole and isoxazole) has been synthesized from the anti-inflammatory drug (nabumetone) as starting compound and their anticancer activity has been evaluated after the good results gained from the molecular docking studies.

## Materials and methods:

### Materials

Nabumetone was obtained from Sigma-Aldrich company (USA), glyoxylic acid monohydrate was obtained from Hopkin and William company (England), hydrazine derivatives (semicarbazide hydrochloride, thiosemicarbazide, 2,4-dinitrophenylhydrazine) and hydroxylamine hydrochloride were obtained from Hangzhou Hyper Chemicals Limited company (China). Commercially available reagents and solvents were used such as (Sigma-Aldrich, England, Spain, China). Melting point was determined by using Stuart electric melting point apparatus (UK). Infrared spectra were determined using a Shimadzu-FT-IR infrared spectrometer and a KBr disc, in the range (4000-400) cm-1. The $^{1}$H-NMR spectra was obtained using a 500 MHz spectrometer and $^{13}$C-NMR spectra was obtained using a 125.60 MHz spectrometer both from the Inova-Varian instrument. The chemical shift was measured in (δ, ppm) using DMSO-d6 as the solvent.

### Methods

### Chemical synthesis:

Scheme of synthesis of new compounds (1, 1a-e & 2a-e) is illustrated below **(Scheme 1).**

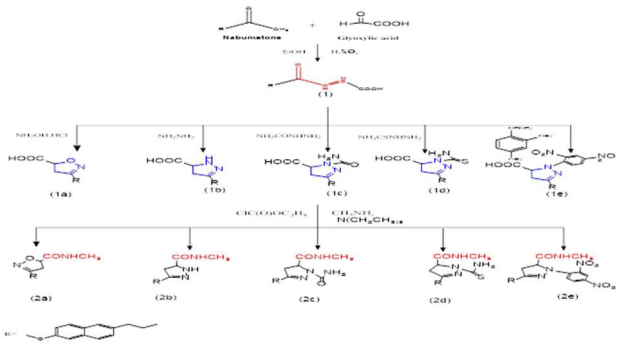

**Scheme (1) Synthesis of intermediate and final compounds.**

### General procedure for the synthesis of chalcone (1):

Nabumetone (1 mmol, 0.228 gm) was dissolved in 10 ml of absolute ethanol. 1.5 ml of concentrated sulfuric acid was added to nabumetone drop by drop and then glyoxylic acid monohydrate (1 mmol, 0.092 gm) was dissolved in absolute ethanol (3ml) solution was mixed with them in the 25 ml round bottom flask. The resulted mixture was refluxed (80 °C) for 24hr. Finally, water was added to the solution and grey powder was obtained upon filtration, wash with water and dried [(14)].

### (E)-6-(6-methoxynaphthalen-2-yl)-4-oxohex-2-enoic acid (1):

Physical characteristics are presented in table (1). **FT-IR spectral data utilizing KBr disc** $\nu$ ($cm^{-1}$) : 3452.70 (OH), 1730.21(C=O), 1718.63(C=O), 1645.33(C=C), 1599.04(C=C aromatic), 1249.91(C-O-$CH_3$).**$^{1}$H-NMR** (500MHz, DMSO-$d_6$), ($\delta, ppm$): 2.62 (t, 2H, $CH_2CH_2$), 3.02 (t, 2H, $CH_2CH_2$), 3.88 (s,3H, $OCH_3$), 6.39 (d, 1H, HC=CH), 7.01 (d, 1H, HC=CH), 7.13-7.92 (m, 6H, Ar-H), 10.63 (Br.s, 1H, OH). **$^{13}$C-NMR** (125.60MHZ, DMSO-$d_6$), ($\delta, ppm$): 30.12 (1C, $CH_2CH_2$), 44.30 (1C, $CH_2CH_2$), 57.15 (1C, $OCH_3$), 131.79(1C, HC=CH), 136.43 (1C, HC=CH), 114.62-153.97

(10 C, Ar-C), 172.73 (1C, C=O of carboxylic acid), 208.13 (1C, C=O of $\propto, \beta$- $unsaturated$ carbonyl system).

**General procedure for the synthesis of (1a):**

Mixture of compound (1) (1mmol, 0.2843 gm) and (1mmol, 0.069 gm) of hydroxylamine hydrochloride was dissolved in 5ml of pyridine. The solution was refluxed for 3hrs. at (115°C), and then cooled, poured on ice hydrochloric acid. Products powder was obtained by filtration, wash with water and dried [15]

**3-(2-(6-methoxynaphthalen-2-yl) ethyl)-4,5-dihydroisoxazole-5-carboxylic acid (1a)**

Physical characteristics are presented in table (1). **FT-IR spectral data utilizing KBr disc** $\nu$ ($cm^{-1}$) : 3414.12 (OH), 1726.35 (C=O), 1606.76 (C=C aromatic and C=N), 1257.63 (C-O-$CH_3$), 1097.53 (C-O of isoxazole ring).**$^1$H-NMR** (500MHz, DMSO-$d_6$), ($\delta, ppm$): 2.43 (t, 2H, $CH_2CH_2$), 2.52, 2.79 (d, 2H, $CH_2$ of isoxazole ring), 2.88 (t, 2H, $CH_2CH_2$), 3.91 (s,3H, $OCH_3$), 6.42 (t, 1H, CH of isoxazole ring), 7.17-7.94 (m, 6H, Ar-H), 10.27 (br.s, 1H, OH). **$^{13}$C-NMR** (125.60MHZ, DMSO-$d_6$), ($\delta, ppm$): 32.00 (1C, $CH_2CH_2$), 37.15 (1C, $CH_2CH_2$), 39.79 (1C, $CH_2$ of isoxazole ring), 57.16 (1C, $OCH_3$), 60.39 (1C, CH of isoxazole ring), 100.44-154.95 (10 C, Ar-C), 172.75 (1C, C=O of carboxylic acid), 180.11 (1C, C=N of isoxazole ring).

**General procedure for the synthesis of (2a)**

Ethyl chloroformate (0.12 ml, 1.25 mmol) was added drop by drop to a suspension of isoxazole product (1a) (0.299 gm, 1 mmole) and triethylamine (0.2 mL, 1.42 mmol) in chloroform (2.5 mL). Throughout the addition process, the temperature was maintained at (5-10°C) and then the resulted solution was stirred continuously for other (30 min.). methylamine solution (40%) (3 mL, 67.6 mmol) was added gradually and the mixture was stirred at room temperature for further (4 hrs.), then extraction with dichloromethane (3x4 ml) was done and the organic layer solvent was evaporated under reduced pressure to collect the required powder [16].

**3-(2-(6-methoxynaphthalen-2-yl) ethyl)-N-methyl-4,5-dihydroisoxazole-5-carboxamide (2a):**

Physical characteristics are presented in table (1). **FT-IR spectral data utilizing KBr disc** $\nu$ ($cm^{-1}$) : 3282.95 (NH), 1724.42 (C=O), 1668.48 (C=N), 1602.90 (C=C aromatic), 1251.84 (C-O-$CH_3$), 1097.53 (C-O of isoxazole ring).**$^1$H-NMR** (500MHz, DMSO-$d_6$), ($\delta, ppm$): 2.45 (t, 2H, $CH_2CH_2$), 2.55, 2.77 (d, 2H, $CH_2$ of isoxazole ring), 2.85 (t, 2H, $CH_2CH_2$), 2.90 (s, 3H, $NCH_3$), 3.87 (s,3H, $OCH_3$), 6.35 (t, 1H, CH of isoxazole ring), 6.39 (br.s, 1H, NH), 7.16-7.97 (m, 6H, Ar-H). **$^{13}$C-NMR** (125.60MHZ, DMSO-$d_6$), ($\delta, ppm$): 29.06 (1C, NCH3), 32.00 (1C, $CH_2CH_2$), 37.15 (1C, $CH_2CH_2$), 39.81 (1C, $CH_2$ of isoxazole ring), 57.16 (1C, $OCH_3$), 60.39 (1C, CH of isoxazole ring), 100.44-154.95 (10 C, Ar-C), 166.00 (1C, C=O of amide), 180.11 (1C, C=N of isoxazole ring).

**General procedure for the synthesis of pyrazole compounds (1b-1e)**

Compound (1) (1mmol, 0.2843 gm) was mixed with one of the different hydrazine derivatives (0.2 ml, 6.24 mmol of hydrazine hydrate, 0.1115 gm, 1mmol of Semicarbazide hydrochloride, 0.0911gm, 1mmol of thiosemicarbazide, 0.1980gm, 1mmol of 2,4-dinitrophenyl hydrazine) and dissolved in (5ml) of dimethyl formamide and 2 drops of glacial acetic acid was added to the mixture. The resulted solution was refluxed for (3 hrs.) at (153°C). Finally, the solution was cooled and poured on crushed ice. The product powder was obtained by filtration [15].

**3-(2-(6-methoxynaphthalen-2-yl) ethyl)-4,5-dihydro-1H-pyrazole-5-carboxylic acid (1b)**

Physical characteristics are presented in table (1). **FT-IR spectral data utilizing KBr disc** $\nu$ ($cm^{-1}$) : 3406.70 (OH), 3379.4(NH of pyrazole ring), 1720.56 (C=O), 1660.77 (C=N), 1612.54 (C=C aromatic), 1257.63 (C-O-$CH_3$).**$^1$H-NMR** (500MHz, DMSO-$d_6$), ($\delta, ppm$): 2.46 (t, 2H, $CH_2CH_2$), 2.51, 2.74 (d, 2H, $CH_2$ of pyrazole ring), 2.88 (t, 2H, $CH_2CH_2$), 3.88 (s,3H, $OCH_3$), 6.42 (t, 1H, CH of pyrazole ring), 7.19-7.97 (m, 6H, Ar-H), 8.68 (br.s, NH of pyrazole ring), 10.63 (br.s, 1H, OH). **$^{13}$C-NMR** (125.60MHZ, DMSO-$d_6$), ($\delta, ppm$): 31.39 (1C, $CH_2CH_2$), 36.23 (1C, $CH_2CH_2$), 39.50 (1C, $CH_2$ of pyrazole ring), 57.14 (1C, $OCH_3$), 60.83 (1C, CH of pyrazole ring), 100.45-154.95 (10 C, Ar-C), 162.78 (1C, C=O of carboxylic acid), 180.11 (1C, C=N of pyrazole ring).

**1-carbamoyl-3-(2-(6-methoxynaphthalen-2-yl) ethyl)-4,5-dihydro-1H-pyrazole-5-carboxylic acid (1c)**

Physical characteristics are presented in table (1). **FT-IR spectral data utilizing KBr disc** $\nu$ ($cm^{-1}$) : 3514.42 (OH), 3425.69 ($NH_2$ asymmetric), 3223.16 ($NH_2$ symmetric), 1722.49 (C=O), 1668.48 (C=N of pyrazole ring and C=O amide), 1604.83 (C=C aromatic), 1257.63 (C-O-$CH_3$).**$^1$H-NMR** (500MHz, DMSO-$d_6$), ($\delta, ppm$): 2.48 (t, 2H, $CH_2CH_2$), 2.51, 2.74 (d, 2H, $CH_2$ of pyrazole ring), 2.89 (t, 2H, $CH_2CH_2$), 3.67 (s,3H, $OCH_3$), 6.41 (t, 1H, CH of pyrazole ring), 7.19-7.97 (m, 6H, Ar-H), 8.65 (br.s, 2H, $NH_2$), 10.25 (br.s, 1H, OH). **$^{13}$C-NMR** (125.60MHZ, DMSO-$d_6$), ($\delta, ppm$): 29.06 (1C, $CH_2CH_2$), 31.23 (1C, $CH_2CH_2$), 36.23 (1C, $CH_2$ of pyrazole ring), 57.16 (1C, $OCH_3$), 60.85 (1C, CH of pyrazole ring), 114.56-153.97 (10 C, Ar-C), 154.95 (1C, C=O of amide) 162.77 (1C, C=O of carboxylic acid), 180.11 (1C, C=N of pyrazole ring).

**1-carbamothioyl-3-(2-(6-methoxynaphthalen-2-yl) ethyl)-4,5-dihydro-1H-pyrazole-5-carboxylic acid (1d)**

Physical characteristics are presented in table (1). **FT-IR spectral data utilizing KBr disc** $\nu$ ($cm^{-1}$) : 3520.21 (OH), 3425.69 ($NH_2$ asymmetric), 3273.31 ($NH_2$ symmetric), 1728.28 (C=O), 1668.48 (C=N of pyrazole ring), 1602.90 (C=C aromatic), 1255.70 (C=S and C-O-$CH_3$).**$^1$H-NMR** (500MHz, DMSO-$d_6$), ($\delta, ppm$): 2.48 (t, 2H, $CH_2CH_2$), 2.51, 2.74 (d, 2H, $CH_2$ of pyrazole ring), 2.92 (t, 2H, $CH_2CH_2$), 3.88 (s,3H, $OCH_3$), 6.41 (t, 1H, CH of pyrazole ring), 7.06-7.97 (m, 6H, Ar-H), 8.39 (br.s, 2H, $NH_2$), 10.61 (br.s, 1H, OH). **$^{13}$C-NMR** (125.60MHZ, DMSO-$d_6$), ($\delta, ppm$): 29.06 (1C, $CH_2CH_2$), 31.24 (1C, $CH_2CH_2$), 36.24 (1C, $CH_2$ of pyrazole ring), 57.16 (1C, $OCH_3$), 60.86 (1C, CH of pyrazole ring), 114.62-153.97 (10 C, Ar-C), 162.78 (1C, C=O of carboxylic acid), 172.75 (1C, C=S), 180.11 (1C, C=N of pyrazole ring).

**1-(2,4-dinitrophenyl)-3-(2-(6-methoxynaphthalen-2-yl) ethyl)-4,5-dihydro-1H-pyrazole-5-carboxylic acid (1e)**

Physical characteristics are presented in table (1). **FT-IR spectral data utilizing KBr disc** $\nu$ ($cm^{-1}$) : 3321.53 (OH), 1732.13 (C=O), 1672.34 (C=N), 1616.40 (C=C aromatic), 1512.24 ($NO_2$ asymmetric), 1311.64 ($NO_2$ symmetric), 1251.84 (C-O-$CH_3$).**$^1$H-NMR** (500MHz, DMSO-$d_6$), ($\delta, ppm$): 2.43 (t, 2H, $CH_2CH_2$), 2.58, 2.74 (d, 2H, $CH_2$ of pyrazole ring), 2.86 (t, 2H, $CH_2CH_2$), 3.88 (s,3H, $OCH_3$), 6.41 (t, 1H, CH of pyrazole ring), 7.21-7.97 (m, 6H, Ar-H), 8.00-8.87 (m, 3H, Ar-H), 10.73 (br.s, 1H, OH). **$^{13}$C-NMR** (125.60MHZ, DMSO-$d_6$), ($\delta, ppm$): 31.23 (1C, $CH_2CH_2$), 31.39 (1C, $CH_2CH_2$), 36.23 (1C, $CH_2$ of pyrazole ring), 57.14 (1C, $OCH_3$),

60.83 (1C, CH of pyrazole ring), 116.44-154.01 (16 C, Ar-C), 162.74 (1C, C=O of carboxylic acid), 180.11 (1C, C=N of pyrazole ring).

**General procedure for the synthesis of amide compounds (2b-2e):**

Ethyl chloroformate (0.12 ml, 1.26 mmol) was drop by drop added to a suspension of one product of pyrazole (1b-1e) (1 mmole) and triethylamine (0.2 mL, 1.42 mmol) in dry chloroform (2.5 mL). Throughout the addition process, the temperature was maintained at (0-5°C) and then the resulted solution was stirred continuously for other (30 min.). methylamine solution (40%) (3 mL, 67.6 mmol) was added gradually and the mixture was stirred at room temperature for further (4 hrs.), then extraction with dichloromethane (3x4 ml) was done and the organic layer solvent was evaporated under reduced pressure to collect the required powder [16].

**3-(2-(6-methoxynaphthalen-2-yl) ethyl)-N-methyl-4,5-dihydro-1H-pyrazole-5-carboxamide (2b)**

Physical characteristics are presented in table (1). **FT-IR spectral data utilizing KBr disc** $\nu$ ($cm^{-1}$) : 3340.82 (NH of pyrazole ring), 3269.45 (NH of amide), 1726.35 (C=O), 1645.33 (C=N), 1600.97 (C=C aromatic), 1251.84 (C-O-$CH_3$).**$^1$H-NMR** (500MHz, DMSO-$d_6$), ($\delta, ppm$): 2.49 (t, 2H, $CH_2CH_2$), 2.55, 2.72 (d, 2H, $CH_2$ of pyrazole ring), 2.75 (t, 2H, $CH_2CH_2$), 2.80 (s, 3H, NCH3), 3.96 (s,3H, $OCH_3$), 5.99 (t, 1H, CH of pyrazole ring), 6.39 (br.s, 1H, NH of amide), 7.06-7.95 (m, 6H, Ar-H), 8.53 (br.s, NH of pyrazole ring). **$^{13}$C-NMR** (125.60MHZ, DMSO-$d_6$), ($\delta, ppm$): 29.06 (1C, NCH3), 39.05 (1C, $CH_2CH_2$), 39.38 (1C, $CH_2CH_2$), 39.55 (1C, $CH_2$ of pyrazole ring), 57.14 (1C, $OCH_3$), 60.83 (1C, CH of pyrazole ring), 100.45-154.95 (10 C, Ar-C), 166.00 (1C, C=O of amide), 180.11 (1C, C=N of pyrazole ring).

**3-(2-(6-methoxynaphthalen-2-yl) ethyl)-N5-methyl-4,5-dihydro-1H-pyrazole-1,5-dicarboxamide (2c)**

Physical characteristics are presented in table (1). **FT-IR spectral data utilizing KBr disc** $\nu$ ($cm^{-1}$) : 3510.56 ($NH_2$ asymmetric), 3373.61 ($NH_2$ symmetric), 3271.38 (NH of amide), 1728.28 (C=O of methyl amide), 1681.98 (C=O of amide), 1631.83 (C=N), 1600.97 (C=C aromatic), 1249.91 (C-O-$CH_3$).**$^1$H-NMR** (500MHz, DMSO-$d_6$), ($\delta, ppm$): 2.53 (t, 2H, $CH_2CH_2$), 2.54, 2.72 (d, 2H, $CH_2$ of pyrazole ring), 2.76 (t, 2H, $CH_2CH_2$), 2.80 (s, 3H, NCH3), 3.86 (s,3H, $OCH_3$), 6.01 (t, 1H, CH of pyrazole ring), 6.38 (br.s, 1H, NH of amide), 7.06-7.95 (m, 6H, Ar-H), 8.57 (br.s,2H, $NH_2$). **$^{13}$C-NMR** (125.60MHZ, DMSO-$d_6$), ($\delta, ppm$): 29.06 (1C, NCH3), 31.23 (1C, $CH_2CH_2$), 36.23 (1C, $CH_2CH_2$), 39.98 (1C, $CH_2$ of pyrazole ring), 57.16 (1C, $OCH_3$), 60.85 (1C, CH of pyrazole ring), 114.56-153.97 (10 C, Ar-C), 154.95 (1C, C=O of pyrazole substituted amide), 166.00 (1C, C=O of amide), 180.11 (1C, C=N of pyrazole ring).

**1-carbamothioyl-3-(2-(6-methoxynaphthalen-2-yl) ethyl)-N-methyl-4,5-dihydro-1H-pyrazole-5-carboxamide (2d)**

Physical characteristics are presented in table (1). **FT-IR spectral data utilizing KBr disc** $\nu$ ($cm^{-1}$) : 3522.13 ($NH_2$ asymmetric), 3468.13 ($NH_2$ symmetric), 3223.16 (NH of amide), 1724.42 (C=O of methyl amide), 1662.69 (C=N), 1604.83 (C=C aromatic), 1255.70 (C-O-$CH_3$ and C=S).**$^1$H-NMR** (500MHz, DMSO-$d_6$), ($\delta, ppm$): 2.43 (t, 2H, $CH_2CH_2$), 2.52, 2.76 (d, 2H, $CH_2$ of pyrazole ring), 2.82 (t, 2H, $CH_2CH_2$), 2.90 (s, 3H, NCH3), 3.88 (s,3H, O_$CH_3$), 6.02 (t, 1H, CH of pyrazole ring), 6.40

(br.s, 1H, NH of amide), 7.05-7.95 (m, 6H, Ar-H), 8.34 (br.s,2H, $NH_2$). **$^{13}$C-NMR** (125.60MHZ, DMSO-$d_6$), $(\delta, ppm)$: 29.06 (1C, NCH3), 29.23 (1C, $CH_2CH_2$), 39.48 (1C, $CH_2CH_2$), 39.64 (1C, $CH_2$ of pyrazole ring), 57.16 (1C, $OCH_3$), 60.86 (1C, CH of pyrazole ring), 114.62-153.97 (10 C, Ar-C), 166.00 (1C, C=O of amide), 172.46 (1C, C=S), 180.11 (1C, C=N of pyrazole ring).

**1-(2,4-dinitrophenyl)-3-(2-(6-methoxynaphthalen-2-yl) ethyl)-N-methyl-4,5-dihydro-1H-pyrazole-5-carboxamide (2e)**

Physical characteristics are presented in table (1). **FT-IR spectral data utilizing KBr disc** $\nu$ ($cm^{-1}$) : 3321.53 (NH), 1730.21 (C=O), 1612.54 (C=N and C=C aromatic), 1512.24 ($NO_2$ asymmetric), 1334.78 ($NO_2$ symmetric), 1253.77 (C-O-$CH_3$).**$^1$H-NMR** (500MHz, DMSO-$d_6$), $(\delta, ppm)$: 2.49 (t, 2H, $CH_2CH_2$), 2.65, 2.73 (d, 2H, $CH_2$ of pyrazole ring), 2.86 (t, 2H, $CH_2CH_2$), 2.89 (s, 3H, $NCH_3$), 3.96 (s,3H, $OCH_3$), 6.02 (t, 1H, CH of pyrazole ring), 6.40 (br.s, 1H, NH), 7.17-7.97 (m, 6H, Ar-H), 8.28-8.84 (m, 3H, Ar-H). **$^{13}$C-NMR** (125.60MHZ, DMSO-$d_6$), $(\delta, ppm)$: 29.06 (1C, $NCH_3$), 31.23 (1C, $CH_2CH_2$), 36.23 (1C, $CH_2CH_2$), 39.82 (1C, $CH_2$ of pyrazole ring), 57.12 (1C, $OCH_3$), 60.83 (1C, CH of pyrazole ring), 114.56-153.97 (16 C, Ar-C), 166.00 (1C, C=O of amide), 180.11 (1C, C=N of pyrazole ring).

**Table (1) The physicochemical characterization data of the synthesized compounds.**

| Melting point | %Yield | Color | M. Wt | Chemical formula | No. |
|---|---|---|---|---|---|
| **99 (dec.*)** | 74.29 | Grey-green | 284.31 | $C_{17}H_{16}O_4$ | 1 |
| | | powder | | | |
| **130-132** | 75.6 | Yellow powder | 299.33 | $C_{17}H_{17}NO_4$ | 1a |
| **153-155** | 84.8 | Faint yellow powder | 298.34 | $C_{17}H_{18}N_2O_3$ | 1b |
| **109-111** | 84.5 | Red-Brown powder | 341.37 | $C_{18}H_{19}N_3O_4$ | 1c |
| **132-134** | 78.8 | Grey powder | 357.43 | $C_{18}H_{19}N_3O_3S$ | 1d |
| **98-101** | 81.6 | Orange powder | 464.43 | $C_{23}H_{20}N_4O_7$ | 1e |
| **101-103** | 74.2 | Brown powder | 312.37 | $C_{18}H_{20}N_2O_3$ | 2a |
| **122-124** | 71.4 | Red powder | 311.39 | $C_{18}H_{21}N_3O_2$ | 2b |
| **169-171** | 69.2 | Brown powder | 354.41 | $C_{19}H_{22}N_4O_3$ | 2c |
| **143-145** | 81.7 | Brown powder | 370.47 | $C_{19}H_{22}N_4O_2S$ | 2d |
| **111-113** | 67.6 | Dark Orange powder | 477.48 | $C_{24}H_{23}N_5O_6$ | 2e |

*dec= decomposed

**Computational methods**

**ADME procedures for the synthesized compounds:**

SwissADME server was used to access ADME (Absorption, Distribution, Metabolism, and Excretion) studies and other physicochemical properties of the newly developed compounds [17]. The chemical structures of the new compounds [1, 1a-e & 2a-e] were drawn using ChemAxon's Marvin JS software. The Swiss ADME tool was used to translate these structures to the SMILE name in order to predict their pharmacokinetic and physicochemical properties. Finally, in these experiments, the BOILED EGG was used to assess passive gastrointestinal absorption and brain penetration, or the polarity and lipophilicity of small molecules [18].

**Molecular docking studies for the synthesized compounds:**

Program of CCDC (Cambridge Crystallographic Data Center) (GOLD) Genetic Optimization for Ligand Docking) (v 5.7.1.) was used to undergo docking studies for the modeled compounds**.**

**Ligands and protein receptor preparation:**

The chemical structures of the newly designed compounds were drawn using the ChemDraw specialist (v.16.0) software at first. Then, using Chem3D (v.16.0) and by undergoing MM2 force field, we were able to minimize the energy of our new compounds. The recently developed ligands were then docked using the three-dimensional structure of the active target: the crystal structure of EGFR protein complexes with erlotinib (PDB code: 4HJO). The receptor was then loaded into GOLD's Hermes module from the protein data bank (PDB) [19]. The receptor (EGFR) was cleaned up by removing all water molecules that are not in the active site (except water molecule (HOH4) within the EGFR kinase receptor. Hydrogen atoms were added to the amino acid residues to ensure proper ionization and tautomeric states.

**Docking methodology:**

CCDC GOLD suite's include, Hermes visualizer package was used to prepare the receptor for docking. For the docking procedure, the protein binding site was identified within the (10 A°) of the reference ligand. The number of produced poses was kept at ten, the top-ranked solution was kept as the default, and the early termination option was disabled. Chemscore kinase was used as a configuration guide. As a scoring function, the piecewise linear potential (ChemPLP) is employed. Finally, the findings were stored as mol.2 files. These findings were analyzed in order to find the optimal interaction between our newly designed ligands and the amino acids of the receptor (EGFR receptor).

**Cell line studies:**

MTT colorimetric assay is used to determine the anticancer activity of the newly designed and synthesized compounds [1,1a-e & 2a-e], on the A549 human lung cancer cell line.

**Cell culture:**

The human A549 lung cancer cell line was obtained from ATCC. It was kept in the tissue culture research laboratory at Mustansiriyah university/college of pharmacy's cell bank.

**Cell line storage and resuscitation:**

Cells were kept at (~80 Cº, for 24hr), under liquid hydrogen. Cells thawing was done at 37 Cº and 10 ml fresh media then was added. The cells

were collected using centrifugation. After that, the addition of 25 ml of fresh medium was done to re-suspend the cells well and they were transferred to a (75 $cm^2$) flask and proliferated there [20].

**Cell maintenance:**

A549 human lung cancer cells were remained in RPMI-1640 Medium (500 ml). Then complete media (50 ml of 10% FBS, 5ml of 1% L-Glutamine, along with 5ml of Penicillin-Streptomycin-Amphotericin B100X as antiseptic) was added. These cells were propagated in 75 $cm^2$ flasks. Incubation of the cells was done in 5% $CO_2$ at 95% humidified air (37 $C^o$). The flasks which contain the A549 cells were passed through sterile conditions when these cells accomplished 90% confluence. Then, a solution of PBS 5ml was utilized in order to wash these cells. After that, these cells were kept (for 2 min) in trypsin solution at 37 $C^o$ in order to ensure the detachment of the cells from the flask bottom. Then, similar quantities of the complete growth media were poured and the resulted suspension of cells was moved into a (50ml) conical tube. Then, centrifuge of the cells was carried out for 3 minutes (1200 rpm). Finally, the supernatant was neglected and resuspension of the cell pellet in the growth media (fresh media) was done. Consequently, cells were counted by the use of Haemocytometer (by the microscope), and utilized as needed [21].

**Cell viability by MTT colorimetric assay:**

MTT colorimetric assay was utilized to determine the cytotoxic effects of newly designed and synthesized compounds [1, 1a-e & 2a-e] on lung cancer cell. The cell suspension (100 µl) was put into 96-well flat-bottom tissue culture plates at concentrations of (5 x $10^3$ cells per well), and then incubated under normal conditions for 24 hours, (4 x $10^3$ cells per well) for 48 hours, and (3 x $10^3$ cells per well) for 72 hours. When the 24hr was finished, treatment of the cells with 50 µM from each of the new synthesized compounds. As the recovery time (24hr, 48hr and 72hr) has been ended, the culture medium of the cells was discarded and incubation of the cultures at 37 $C^o$ for 4hr with a medium which include 30 µl of MTT solution (3mg/ml of MTT powder in PBS) was done. The medium was removed once the 4 hours were up by flipping the paper and turning it over. The control wells were then supplied with (100 µl) of growth media. Then 100 µl of DMSO was poured into each well, which was then kept at room temperature for 15-20 minutes in a dark location[22]. The MTT assay was carried out in triplicate, and the optical density of each plate was measured using a Multiscan Reader at a transmission wavelength (520-600 nm). We can calculate the rate of inhibition of cell growth (cytotoxicity percentage) by using the following equation:

[Inhibition Rate percentage= (A-B/A)*100]

Where [A, and B] represent the optical density of control & tested compounds [23].

**$IC_{50}$ (half-maximal inhibitory concentration) determination:**

Dose-response curve can be used to obtain the tested compounds $IC_{50}$. With regard to the MTT assay (*in vitro)*, the $IC_{50}$ can be defined as the needed concentration of the tested newly synthesized compounds [1, 1a-e & 2a-e] to get 50% cell inhibition. The concentration ranges of compounds [1, 1a, 1b, 1c, 1d, 1e, 2a, 2b, 2c, 2d & 2e] utilized to estimate the $IC_{50}$ values was (100, 50, 25, 12.5, 6.25, 3.125, 1.562, 0.781, 0.390 & 0.195 µM) [24].

**Statistical analysis:**

Nonlinear curve fitting software prism pad software was used to analyze the MTT assay and $IC_{50}$ data. One-way ANOVA with Tukey (prism pad software) were utilized to compare between all of the groups which are included in the same plate of MTT ($p < 0.05$ were considered as statistically significant) [25].

**Results and discussion:**

**ADME results interpretation:**

Results of ADME study of the newly designed compounds are represented in table (2). SwissADME include many parameters comprise the topological polar surface area (TPSA), refer to the ability of drugs to penetrate cells, compounds with TPSA *lower than* $140Å^2$ mean high permeability and bioavailability [26] . Results showed that most compounds have TPSA $< 140Å^2$ range from (59.92-120.24) $Å^2$ except compounds [1e & 2e] give TPSA in range (153.77-145.57) $Å^2$ respectively. However, the lipophilicity (log $P_{o/w}$) of all compounds satisfied the typical range [log $P_{o/w} < 5$]. Other parameter is molar solubility in water (log S) ranges from soluble to moderate solubility, except poor solubility for compounds [1e, 2b & 2e]. GIT absorption of most ligands was high this predict that compounds passively and highly absorbed except compounds [1e & 2e]. Moreover, the bioavailability score of compounds ranges from [0.55-0.85] except poor bioavailability for compound [1e] was [0.11] [27].

**Table (2) Intermediate and target compound ADME findings**

| Comp. | H-donor | H-acceptor | MR | TPSA | GI Abs. | BBB permeability | Bio-availability | Lipinski violation |
|---|---|---|---|---|---|---|---|---|
| **1** | 1 | 4 | 80.94 | 63.6 | High | Yes | 0.85 | 0 |
| **1a** | 1 | 5 | 87.19 | 68.12 | High | Yes | 0.85 | 0 |
| **1b** | 2 | 4 | 92.83 | 70.92 | High | Yes | 0.85 | 0 |
| **1c** | 2 | 5 | 101.02 | 105.22 | High | No | 0.56 | 0 |
| **1d** | 2 | 4 | 108.23 | 120.24 | High | No | 0.56 | 0 |
| **1e** | 1 | 8 | 135.61 | 153.77 | Low | No | 0.11 | 1[N or O >10] |
| **2a** | 1 | 4 | 93.23 | 59.92 | High | Yes | 0.55 | 0 |
| **2b** | 2 | 3 | 98.86 | 62.72 | High | Yes | 0.55 | 0 |
| **2c** | 2 | 4 | 107.06 | 97.02 | High | No | 0.55 | 0 |

| | | | | | | | | |
|---|---|---|---|---|---|---|---|---|
| **2d** | 2 | 3 | 114.26 | 112.04 | High | No | 0.55 | 0 |
| **2e** | 1 | 7 | 148.57 | 145.57 | Low | No | 0.55 | 1[N or O >10] |

**Explanation and discussion of the results of molecular docking studies:**

Results of docking study of the newly designed compounds are represented in figures (1, 2& 3) and tables (3). Docking data revealed that all the designed ligands (1, 1a-e & 2a-e) demonstrate good binding energies in the active pocket of the receptor and expected promising interaction with EGFR, and ER-α protein, as it binds to the amino acids (AAs) residue of the active site through H-bonds along with other short contacts that reinforce the binding. In general, pyrazole derivatives show best results than chalcone and isoxazole derivatives, However, there is a remarkable correlation and compatibility between the experimental findings and our docking (***In Vitro)*** results. Generally, the results of docking revealed that pyrazole derivative compound (2e) with EGFR protein exhibit the maximum PLP fitness value of (97.11) and H-bonding with two amino acids in which Cys773 form H-bond with carbonyl of the amide group, and nitro group with Met769 as depicted in table (3) and figure (1) beside other short contact. Compound (1e) give (92.07) PLP fitness value and form H-bond through carbonyl of the carboxylic group with Arg817 in comparsion with the standard drug erlotinib (94.84) shown in figure(2) [(28)].

**Table (3) The binding energies of nabumetone derivatives and erlotinib, a conventional medication, docked with EGFR.**

| **Compound** | **EGFR binding energy (PLP fitness)** | **Amino acids includes in H-bonding** | **Amino acids includes in short contact** |
|---|---|---|---|
| **1** | 72.8 | Met769 | Met742, Val702(5), Asp831 |
| **1a** | 69.27 | ------- | Val702(5), Met742, Leu764, HOH-AM1 |
| **1b** | 71.26 | Thr830, Asp831(2), Lys721 | Lys721, Thr830, Asp831(2), Val702 |
| **1c** | 76.66 | Cys773, ,Met769 | Cys773, ,Met769, Leu694(2), Leu769, Val702(4), |
| **1d** | 77.69 | Met769 | Met769, Cys773, Leu694, Val702(4), Asp831(2), Leu753 |
| **1e** | 92.07 | Arg817 | Arg817, Lys721, Met742,Thr830 through $H_2O$ bridge HOH-AM1, Val702, Phe832 |
| **2a** | 72.69 | Asp831, Thr830(2) | Asp831, Thr830 through $H_2O$ bridge, HOH-AM1, Val702, |

| | | | |
|---|---|---|---|
| **2b** | 75.15 | Asp831(2), Thr830, Lys721 | Asp831(4), Thr830,Gly772 |
| **2c** | 83.37 | Gln767, Met769, HOH-AM1 | Met769, Gln767, Val702(4),Leu820, Asp831, Leu753 |
| **2d** | 78.9 | Leu694 | Leu694(3), Cys773, Val702(2), Leu820, Asp831 |
| **2e** | 97.11 | Cys773, Met769 | Cys773(2) *, Leu753, Leu694,Asp831, Val702(3) |
| **Erlotinib** | 94.84 | Met769, Lys721 | Leu694, Met769, Lys721, Lys704, HOH-AM1 |

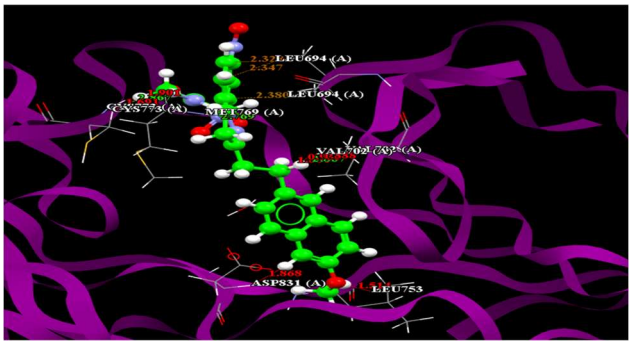


**Figure (1) The compound's [2e] The EGFR receptor's H-bond and short-contact interaction profile (PDB code: 4HJO). Contact between the compound and the amino acid residues [Cys773, Met769] through hydrogen bonds is shown in green, whereas short contact is represented in red.**

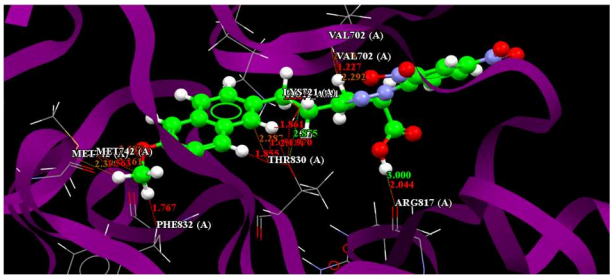


**Figure (2) The compound's [1e] The EGFR receptor's H-bond and short-contact interaction profile (PDB code: 4HJO). Contact between the compound and the amino acid residue [Arg817] through an H-bond is shown in green, whereas short contact is represented in red.**

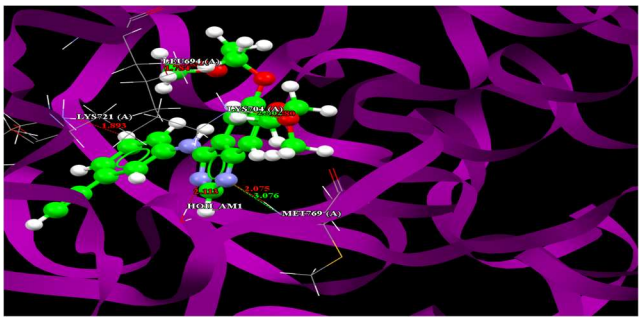


**Figure (3) The conventional medication Erlotinib's H-bond and short contact interaction profile with the EGFR receptor (PDB code: 4HJO). H-bond contact between erlotinib and amino acid residues [Met769, Lys704] is shown in green, whereas short contact is represented in red.**

**Results of cytotoxicity studies: Cytotoxicity assay results of compounds against lung cancer cell line (A549):**

$IC_{50}$ values of the synthesized compounds were determined using the MTT assay. The assay was done in 96-well flat plates to a range of concentrations (100 – 0.15 µM) of the synthesized compounds [1,1a-e & 2a-e] and the $IC_{50}$ values were obtained after treating the cells with the compounds for 72 hrs. The resulted $IC_{50}$ values of these compounds were compared with

reference antitumor drug erlotinib. The dose-response curves were generated by Prism Pad 8.1 using nonlinear regression analysis for the synthesized compounds in A549 cells are shown in below figures (4, 5& 6). The $IC_{50}$ values were demonstrated in table (4) below [29].

**Table (4) The $IC_{50}$ values of the effective compounds (1e, 2e) and erlotinib as standard against lung cancer cell line (A549).**

| Compound | $IC_{50}$ values µM |
|---|---|
| 1e | 27.61 |
| **2e** | **21.62** |
| Erlotinib | 24.6 |

The newly synthesized compounds [1e & 2e] exhibited potential anticancer activity, according to the above results. The most significant cytotoxic effect was for compound [2e], which had an $IC_{50}$ value of 21.62 µM, which makes it may be more active than the reference drug erlotinib, which had an $IC_{50}$ value of 24.6 µM. While compound [1e] has slightly higher $IC_{50}$ value 27.61 µM than erlotinib which means it had slightly lower anticancer activity than the standard.

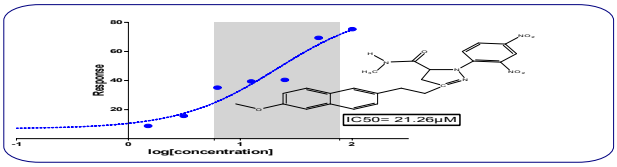


**Figure (4): $IC_{50}$ dose-response curves for (2e).**

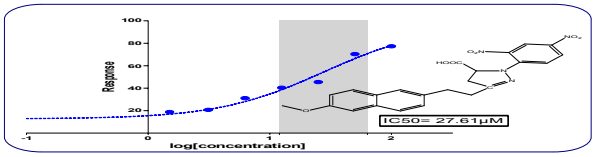


**Figure (5): $IC_{50}$ dose-response curves for (1e).**

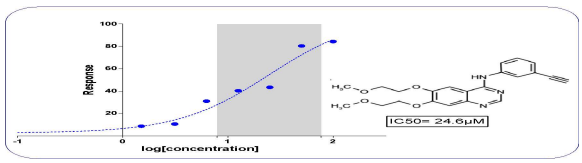


**Figure (6): $IC_{50}$ dose-response curves for Erlotinib (Control).**

**Estimation of percentage (%) of lung cancer (A549) cell death using erlotinib and as standard drugs in comparison with the tested compounds:**

The MTT assay was used on human lung (A549) cells to measure the percentage (%) of cell death of the studied compounds [1,1a-e & 2a-e] at (30 & 35µM) for A549. Erlotinib was used as the standard reference at the same concentration, at varied contact periods of 24, 48, and 72 hours. The results demonstrate the mean absorbance ± SEM of 3 independent experiments using Prism Pad 8.1 software to draw the dose time response Versus percent (%) of cell death graph line which is shown in figure (7). The findings demonstrated that the percentage of cancer cells that die is associated with time increasing from 24 to 72 hours. When compared to standard, all of the tested compounds reveal significant variation in cell death response. With lung cancer cell line compound [1e] give (77.34%) of cell death, while compound [2e] give (75.34%) of cell death. These results revealed that when compared to standard drug erlotinib was (84.34%) still have lower percentage of cell death but good activity.

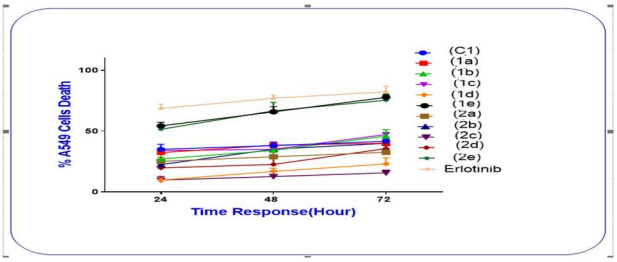


**Figure (7): *In vitro* % cell death of the lung cancer (A549) cells was detected by MTT assay.**

**Conclusion:**

All synthesized compounds were substantially absorbed from the GIT according to ADME studies except compounds (1e & 2e),

furthermore; docking investigations revealed that the in vitro results and docking studies were highly compatible since 1e & 2e compounds exert strong to moderate antiproliferative as compared to the standard drug.

**Conflict of interest:**

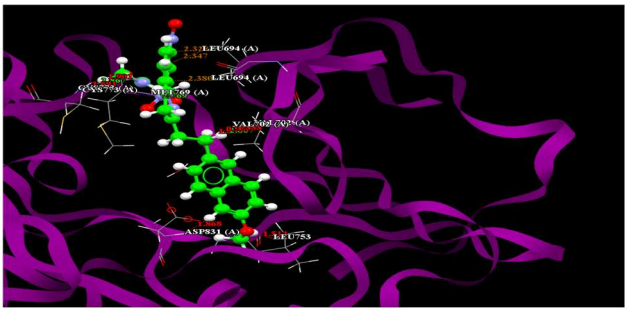


**Figure (8) The compound's [2e] H-bond and short contact interaction profile with the EGFR receptor (PDB code: 4HJO).**

**Acknowledgments:**

For their assistance and support, the authors are thankful to the chairman and members of the department of pharmaceutical chemistry and the department of pharmacology and toxicology at Mustansiriyah University's college of pharmacy.

**References:**

1. J. Chavda, H. Bhatt, Systemic Review on B-RafV600E Mutation as Potential Therapeutic Target for the Treatment of Cancer, European Journal of Medicinal Chemistry, https:// doi.org/10.1016/j.ejmech.2020.112675.
2. Patel GM, Patel JD. Single Core Osmotic Pump (SCOP): Development of Single Layer Osmotic controlled release tablet for poorly soluble drug. J Pharm Technol Drug Res. 2012;4(1):1–9. Doi: 10.7243/2050-120x-1-1.
3. Mahdy NE, Rahman AARA, Hassan HA. Cytotoxic Drugs Safety Guidelines: Its Effect on Awareness and Safe Handling Practices of Oncology Nurses. IOSR J Nurs Heal Sci. 2017;06(03):22–33. Doi: 10.9790/1959-0603032233.
4. Chang J, Ren H, Zhao M, et al. Development of a series of novel 4-anlinoquinazoline derivatives possessing quinazoline skeleton: Design, synthesis, EGFR kinase inhibitory efficacy, and evaluation of anticancer activities in vitro. Eur J Med Chem. 2017;138:669–88. Doi: 10.1016/j.ejmech.2017.07.005.
5. Faivre S, Djelloul S, Raymond E. New Paradigms in Anticancer Therapy : Targeting Multiple Signaling Pathways With Kinase Inhibitors. Semin Oncol 33:407-420 © 2006 Elsevier Inc. 2006;407–20. Doi: 10.1053/j.seminoncol.2006.04.005
6. Mujeeb Ur Rahman, G. Jeyabalan, Pankaj Saraswat, et al. Quinazolines and anticancer activity: A current perspectives, Synthetic Communications, 47:5, 379-408, Doi: 10.1080/00397911.2016.1269926.
7. El-sattar NEAA, Badawy EHK. Synthesis of Some Pyrimidine , Pyrazole , and Pyridine Derivatives and Their Reactivity Descriptors. J Chem. 2018;2018:11. Doi: https://doi.org/10.1155/2018/8795061.
8. Marquina S, Maldonado-Santiago M, Sánchez-Carranza JN, et al. Design, synthesis and QSAR study of 2′-hydroxy-4′-alkoxy chalcone derivatives that exert cytotoxic activity by the mitochondrial apoptotic pathway. Bioorganic Med Chem. 2019;27(1):43–54. Doi: 10.1016/j.bmc.2018.10.045.
9. Burmaoglu S, Ozcan S, Balcioglu S, et al. Synthesis, biological evaluation and

molecular docking studies of bis-chalcone derivatives as xanthine oxidase inhibitors and anticancer agents. Bioorg Chem. 2019;91:103149. Doi: 10.1016/j.bioorg.2019.103149.

10. Higgs J, Wasowski C, Marcos A, et al. Chalcone derivatives: synthesis, in vitro and in vivo evaluation of their anti-anxiety, anti-depression and analgesic effects. Heliyon. 2019;5(3). Doi: 10.1016/j.heliyon.2019.e01376.
11. Karrouchi K, Radi S, Ramli Y, et al. Synthesis and pharmacological activities of Pyrazole derivatives: A review. Vol. 23, Molecules. 2018. 1–85. Doi: 10.3390/molecules23010134.
12. Khan MF, Alam MM, Verma G, et al. The therapeutic voyage of pyrazole and its analogs: A review.Eur J Med Chem. 2016;120:170–201. Doi: 10.1016/j.ejmech.2016.04.077.
13. Agrawal N, Mishra P. CHEMISTRY The synthetic and therapeutic expedition of isoxazole and its analogs. Med Chem Res. 2018;1309–44. Doi: 10.1007/s00044-018-2152-6.
14. Amarasekara AS, Ha U. Acid catalyzed aldol condensations of ketones with glyoxylic acid: A simple single-step synthesis of 4-oxo-2,5-heptdienedioic acids. Synthetic Communications.2018:48 :(19):2533-2538. Doi: 10.1080/00397911.2018.1511998.
15. Salem MAI, Marzouk MI, El-Kazak AM. Synthesis and characterization of some new coumarins with in vitro antitumor and antioxidant activity and high protective effects against DNA damage. Molecules. 2016;21(2):20-1. Doi: 10.3390/molecules21020249.
16. Mahdi MF, Raauf AMR, Rzoqi SS. Synthesis, characterization and antimicrobial study of new nalidixic acid mannich base derivatives. Der Pharma Chem. 2016;8(19):424–32.
17. Daina A, Michielin O, Zoete V. SwissADME: A free web tool to evaluate pharmacokinetics, drug-likeness and medicinal chemistry friendliness of small molecules. Sci Rep. 2017;7:1–13. Doi: 10.1038/srep42717
18. Daina A, Zoete V. A BOILED-Egg To Predict Gastrointestinal Absorption and Brain Penetration of Small Molecules. ChemMedChem. 2016;1117–21. Doi: 10.1002/cmdc.201600182
19. Park, J.H., et al. Erlotinib binds both inactive and active conformations of the EGFR tyrosine kinase domain. Biochemical Journal, 2012. 448(Pt 3): p.417. Doi: 10.1042/BJ20121513.
20. Shi Y, Tang B, Yu PW, et al. Autophagy Protects against Oxaliplatin-Induced Cell Death via ER Stress and ROS in Caco-2 Cells. PLoS One. 2012;7(11):1–8. Doi: 10.1371/journal.pone.0051076.
21. Kaplan F, di Lenardo I. Big Data of the Past. Front Digit Humanit. 2017;4(:1–12. Doi: 10.3389/fdigh.2017.00012.
22. Chang J, Ren H, Zhao M, et al. Development of a series of novel 4-anlinoquinazoline derivatives possessing quinazoline skeleton: Design, synthesis, EGFR kinase inhibitory efficacy, and evaluation of anticancer activities in vitro. Eur J Med Chem. 2017;138:669–88. Doi: 10.1016/j.ejmech.2017.07.005.
23. Shaaban OG, Abd El Razik HA, A Shams

El-Dine SED, et al. Purines and triazolo[4,3-e]purines containing pyrazole moiety as potential anticancer and antioxidant agents. Future Med Chem. 2018;10(12):1449–64. Doi: 10.4155/fmc-2017-0227

24. Sebaugh JL. Guidelines for accurate EC50/IC50 estimation. Pharm Stat. 2011;10(2):128–34. Doi: 10.1002/pst.426.
25. Wabdan AK, Mahdi MF, Khan AK. Molecular docking, synthesis and adme studies of new pyrazoline derivatives as potential anticancer agents. Egypt J Chem. 2021;64(8):4311–22. Doi: 10.21608/ejchem.2021.64042.3377.
26. Pajouhesh H, Lenz GR. Medicinal chemical properties of successful central nervous system drugs. NeuroRx. 2005;2(4):541–53. Doi: 10.1602/neurorx.2.4.541.
27. Taha, Duha E., Ayad MR Raauf, and Karima F. Ali. "Design, Synthesis,Characterization, Biological Activity and ADME Study of New 5-arylidene-4-Thiazolidinones Derivatives Having." *Al-Mustansiriyah Journal of Pharmaceutical Sciences (AJPS)* 19.4 (2019): 77-88. Doi: https://doi.org/10.32947/ajps.19.04.0421.
28. Adnan, Abdul Muhaimen Amjed, Monther Faisal Mahdi, and Ayad Kareem Khan. "New 2-Methyl Benzimidazole derivatives bearing 4-Thiazolidinone heterocyclic rings: Synthesis, Preliminary pharmacological assessment and docking studies." *Research Journal of Pharmacy and Technology* 14.3 (2021): 1515-1520. Doi: 10.5958/0974-360X.2021.00269.9.
29. Mohammed, Ahmed Wahhab, Inam Samih Arif, and Ghaith Ali Jasim. "The Cytotoxic Effect of Metformin on RD Cell Line." *Al-Mustansiriyah Journal of Pharmaceutical Sciences (AJPS)* 19.1 (2019): 85-94. Doi: https://doi.org/10.32947/ajps.19.01.03